

PL ISSN 0033-2097, e-ISSN 2449-9544

7'2021



# PRZEGLĄD ELEKTROTECHNICZNY

ROK XCVII

WYDAWNICTWO  
**SIGMA-NOT**



cena 58 zł  
(w tym 8% VAT)



*100-lecie Wydziału Elektrycznego Politechniki Warszawskiej  
artykuł historyczny – str. 138*

Contents

01	<b>Leszek S. CZARNECKI, Motab ALMOUSA</b> - Conversion of Fixed-Parameters Compensator in Four-Wire System with Nonsinusoidal Voltage Into Adaptive Compensator	1
02	<b>Sompod WONGKHEAD, Satean TUNYASRIRUT</b> - Implementation of a DSP- TMS320F28335 Based State Feedback with Optimal Design of PI Controller for a Speed of BLDC Motor by Ant Colony Optimization	7
03	<b>Salima ASANOVA, Murodbek SAFARALIEV, Nurlan ASKARBEK, Sergey SEMENENKO, Erkin AKTAEV, Anastasia KOVALEVA, Egor LYUKHANOV, Elena STAYMOVA</b> - Calculation of power losses at given loads and source voltage in radial networks of 35 kV and above by hierarchical-multilevel structured topology representation	13
04	<b>Salah Alkurwy</b> - Design and Implementation of Parallel Multiplier Using Two Split Circuits	19
05	<b>Chuthong SUMMATTA, Weera RATTANANGAM</b> - The Improvement of a Fail-safe Counter for Low-speed Detection	23
06	<b>Dmytro SNIZHKO, Anatoliy BYKH, Baohua LOU, Guobao XU</b> - "Pulsar" Photon Counter in Electrogenerated Chemiluminescent Measurements	29
07	<b>Thanat NONTHAPUTHA, Montree KUMNGERN</b> - CMOS Programmable PID Controller Circuit Based Analogue Switches	39
08	<b>Djamel Eddine CHAOUCH, Hocine Abdelhak AZZEDDINE, Ahmed LARBAOUI, Zoubir AHMED-FOITIH</b> - SRF Control Strategy based on STFIS Controllers For Single-Stage Four-Leg Transformerless Inverter for Grid-Connected PV system	42
09	<b>Andrii Bereziuk, Oleksiy Karlov, Roman Kryshchuk, Ihor Garasymchuk, Pavlo Potapskyi, Mykola Vusatyi</b> - Energy parameters of induction heat generator with branched heat exchanger for production of environmentally friendly coolant	48
10	<b>Khalid Subhi Ahmad, Mohamad Zoinol Abidin Abd. Aziz</b> - Pattern reconfigurable planar antenna array based on two circular defected ground structure	52
11	<b>Mowafak K. Mohsen</b> - Using EBG to Enhance Directivity, Efficiency, and Back Lobe Reduction of a Microstrip Patch Antenna	56
12	<b>Benaissa Tahar, Mahi Djillali, Halbaoui Khaled</b> - Maximum Power Point Tracking under simplified sliding mode control based DC-DC boost converters	60
13	<b>Rahul Kumar Verma, Anubhav Kumar, R.L Yadava</b> - WI-FI Reconfigurable Dual Band Microstrip MIMO Antenna for 5G and WI-FI / WLAN Applications	66
14	<b>Somchai ARUNRUNGRUSMI, Wittawat POONTHONG, Apidat SONGRUK, Narong MUNGKUNG, Nutte THUNGSUK, Kongsak ANUNTAHIRANRATH, and Toshifumi YUJI</b> - Application of Atmospheric-pressure Non-equilibrium Microwave Discharge Plasma for Decomposition of Sodium Dodecyl Sulfate in Aqueous Solution	72
15	<b>Irina Gunko, Valerii Hraniak, Vitalii Yaropud, Ihor Kupchuk, Volodymyr Rutkevych</b> - Optical sensor of harmful air impurity concentration	76
16	<b>Reda KARA, Abdelhalim TLEMCANI, Nawel HASSAOUI</b> - Interval type-2 fuzzy logic controller based DPC-SVM algorithm for PWM rectifier	80
17	<b>Aleksandra SKUZA, Marek SUPRONIUK, Stanisław ZIEMIANEK</b> - Influence of current leakage phenomenon on impedance measurements in high voltage networks).	85
18	<b>Bogdan PERKA</b> - Review of heat flow modeling methods in electric wires	90
19	<b>Andriy CZABAN, Vitaliy LEVONIUK, Radosław FIGURA</b> - The mathematical model of high voltage switch as an element of a power system	94
20	<b>Marek LEŚNIEWICZ</b> - Contemporary methods and systems of clock cycle generation with high accuracy and stability and negligible jitter	98
21	<b>Imen SAIDI, 2. Nahla TOUATI</b> - Sliding mode control to stabilization of nonlinear Underactuated mechanical systems	106
22	<b>Ferdous S. Azad, Golam Sarowar, Istiak Ahmed</b> - Development of single-phase single switch AC-DC Zeta converter for improved power quality	110
23	<b>Dominika KACZOROWSKA, Przemysław JANIK, Łukasz JASIŃSKI, Jacek REZMER, Vishnu SURESH</b> - Power flow control algorithm in a microgrid with energy storage	116
24	<b>Rafał OWCZARCZAK, Paweł ŻYLKA</b> - Harvesting energii jako metoda bezbaterijnego zasilania zdalnych układów czujnikowych w budynkach z systemem zarządzania BMS	120
25	<b>Ali Hasan Mousa, MOHD AZLISHAH BIN OTHMAN, Mohamed Zoinol Abidin, Ayman Mohammed Ibrahim</b> - Sierpinski MIMO Antenna for 5G Applications	126
26	<b>J. Samson Immanuel, *G. Manoj, Shajin Prince, H. Victor Du John</b> - Analysis of FPGA accelerator architecture for Fast Statistical Convolutional Neural Network in real time Emotional Recognition System	132
27	<b>Ivan SOLOVEI</b> - Investigation of the influence of microwave irradiation of sowing material on grain yield	135
28	<b>Przemysław SADŁOWSKI, Jerzy HICKIEWICZ</b> - 100th anniversary of the Faculty of Electrical Engineering of the Warsaw University of Technology	138

## Optical sensor of harmful air impurity concentration

**Abstract.** It is shown that to solve the problem of ensuring acceptable sanitary conditions in livestock premises while minimizing energy costs, it is advisable to use an automated exhaust ventilation system with control over the contour of the allowable concentration of harmful atmospheric impurities. The proposed block diagram of the sensor concentration of harmful impurities in the air, suitable for operation in conjunction with an automated ventilation system. Its mathematical model and transformation equation are obtained. It is shown that in the measurement range, which corresponds to the change of controlled impurities in the range from zero to the maximum allowable concentration, the static characteristic of the proposed sensor can be approximated by a linear function without significant additional methodological error.

**Streszczenie.** Wykazano, że w celu rozwiązania problemu zapewnienia akceptowalnych warunków sanitarnych w pomieszczeniach inwentarskich przy jednoczesnym zminimalizowaniu kosztów energii wskazane jest zastosowanie automatycznego systemu wentylacji wyciągowej z kontrolą konturu dopuszczalnego stężenia szkodliwych zanieczyszczeń atmosferycznych. Proponowany schemat blokowy czujnika stężenia szkodliwych zanieczyszczeń w powietrzu, przystosowany do współpracy z systemem wentylacji. Wykazano, że w zakresie pomiarowym, który odpowiada zmianie kontrolowanych zanieczyszczeń w zakresie od zera do maksymalnego dopuszczalnego stężenia, charakterystykę statyczną proponowanego czujnika można aproksymować funkcją liniową bez znacznego dodatkowego błędu metodologicznego. (**Optyczny czujnik stężenia szkodliwych zanieczyszczeń w powietrzu**)

**Keywords:** measurement, harmful impurities, air, optical measurement method.

**Słowa kluczowe:** czujnik zanieczyszczenia powietrza, kontrola zanieczyszczenia powietrza

### Introduction

Today, the effective functioning of farms in modern conditions requires development and implementation of technologies that meet international standards and reduce excessive energy losses [1, 2].

At their location places, animals inevitably generate harmful gases, among which carbon dioxide, ammonia and hydrogen sulfide are the most typical ones. Maximum permissible concentrations of these impurities in the atmosphere of livestock facilities are strictly regulated, and their excess can not only cause the deterioration in the animals' productivity, but also their mass death [3].

Arrangement of a forced exhaust ventilation system represents a typical approach to solving the problem of such atmospheric impurities' excessive concentration. However, operation of ventilation systems requires a significant power consumption, the amount of which is proportional to its performance. And this is the winter season, when this problem is especially acute: on the one hand, the rate of contaminants' generation increases due to the animals' being held indoors permanently, and on the other hand – the ventilation system's operating costs are complemented by the costs of the living area's heating, which also increase with the growth in the productivity of the latter [4, 5].

In view of the foregoing, apparent is the need to maintain the atmospheric concentration of these contaminants at a certain "optimal" level. And since the ability to ensure an optimal concentration of these impurities is significantly limited today by the lack of high-precision concentration sensors suitable for long-term real-time operation as part of an automated ventilation control circuit [6, 7], one can state for sure that designing of such sensors is a relevant research and application-related task.

### Setting the task

Calometric, nephelometric, photometric and others are the most common methods for laboratory analysis of air samples containing harmful gases [8].

The calometric method is the most common and accurate one, which consists in generation of solutions stained with a harmful gas, followed by assessment of the degree of light flux solution's absorption with a photoelectrocalorimeter [9]. The nephelometric method consists in determining the

intensity of sediment formation after investigated harmful gas's interaction with certain chemicals.

To solve this problem, it is necessary to measure the concentration of impurities on real-time basis. Therefore, the use of chemical-based methods is impractical [10]. Hence, as a basic method for implementation of harmful impurities' concentration sensor to be suitable for use in conjunction with the automatic system of monitoring the livestock premises' ventilation, the use of an optical method [11] of measuring the concentration is proposed. This method will ensure an intermediate measurement of attenuation of transmitted electromagnetic wave's amplitude, the frequency of which is going to correspond to the investigated impurity's absorption band.

### Analysing the ways of problem solution

To implement this task, an optical sensor for concentration of harmful impurities is offered, the block diagram of which is shown in Fig. 1.

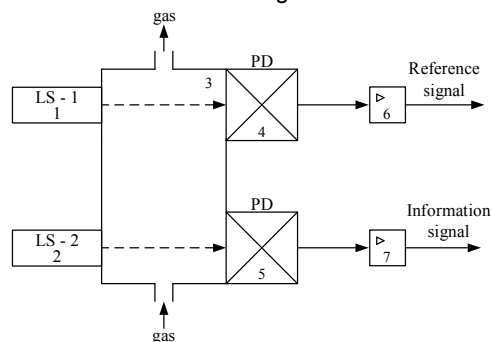


Fig.1. Block diagram of the optical sensor for harmful impurities' concentration

The device operates as follows. The first radiation source 1 emits a narrow-spectrum optical beam that does not correspond to the absorption lines of the analyzed gas's components. The second radiation source 2 emits a narrow-spectrum optical beam corresponding to the absorption lines of the analyzed gas's components. Passing through shielded cuvette 3, the rays from the output of the first 1 and the second 2 radiation sources fall on the inputs, respectively, of the first 4 and second 5 photodetectors. Cuvette 3 is filled with the test gas (which can be pumped forcibly or be introduced by natural convection).

The light beam from the exit of the first radiation source 1, when passing through cuvette 3, will be attenuated due to non-absolute transparency of the test gas. Hence, the transparency ratio of the test gas's optical medium can be determined as follows:

$$(1) \quad \alpha = \frac{F_1}{F_0},$$

where  $F_0$  is the luminous flux of the beam at the output of the first 1 and second 2 radiation sources;  $F_1$  – the ray's luminous flux at the input of the first photodetector 4.

When passing through cuvette 3, the light beam from the output of the second radiation source 2 is additionally (not accounting for the test gas's transparency) attenuated in accordance with Bouguer-Lambert-Beer's law:

$$(2) \quad F_m(c) = F_0 e^{-\varepsilon c d},$$

where  $F_m$  – is the theoretical light beam at the entrance of the second photodetector 5;  $\varepsilon$  – is the molar monochromatic absorption coefficient;  $c$  – is the molar concentration;  $d$  is the distance traveled by the beam.

Given that the beam from the second radiation source 2 will also suffer attenuation through the environment's non-absolute transparency, the actual light output beam at the second sensor's entrance 5 will be calculated as follows [12]:

$$(3) \quad F_2(c) = \alpha F_0 e^{-\varepsilon c d}.$$

In the first 4 and second 5 photodetectors, the intensity of the luminous flux is converted at the level of direct voltage supplied, respectively, to the inputs of the first 6 and the second 7 normalizing amplifiers [13, 14], where they are amplified to the level suitable for further analysis.

It is proposed to use a connected pair of photodiode-operational amplifiers as photodetectors. Fig. 2 shows its electrical schematic diagram, and Fig. 2 – its equivalent substitution scheme.

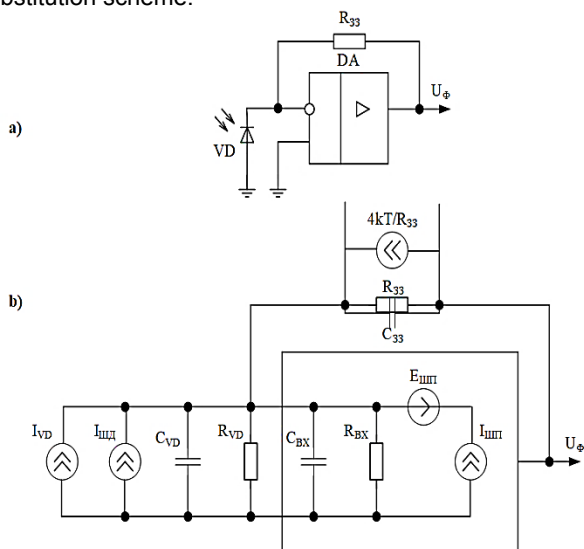


Fig. 2. Photodetector based on the photodiode-operational amplifier's pair

In this circuit, VD photodiode acts as a current generator, and operational amplifier DA [14] converts this current into voltage. The dependence of the current that flows through the photodiode on the irradiation flux is described by expression [15].

$$(4) \quad I_{VD} = \frac{FSI_0}{\sqrt{1 + (\omega\tau_{VD})^2}} - I_S \left( e^{\frac{e_e U_{VD}}{kT}} - 1 \right),$$

where  $I_{VD}$  is the photodiode's current;  $S_{I0}$  – the photodiode's current sensitivity to selected irradiation spectrum;  $F$  is the

luminous flux;  $I_S$  – is the photodiode's dark current;  $U_{VD}$  – the voltage drop on the photodiode;  $T$  – the absolute temperature;  $k$  is the Boltzmann constant;  $e_e$  is the electron charge;  $\omega$  is the cyclic frequency of the modulated irradiation flux;  $\tau_{VD}$  is the photodiode's temporal constant, which depends on the values of  $R_{VD}$  photodiode's internal resistance,  $C_{VD}$  photodiode's parasitic capacitance and Dissemination and minority charge carrier's discharge time.

That said, the output voltage of the photosensor of proposed design, considering the noise voltage, zero offset and the difference of input currents may be described as [16]:

$$(5) \quad U_{\Phi} = \frac{I_{VD} R_{33}}{1 + \frac{R_{33}}{K R_{BX}} + \frac{1}{K}} + \Delta I \cdot R_{33} + U_{3M} + U_{III},$$

where  $K$  is the operational amplifier's transmission factor;  $R_{BX}$  – the operational amplifier's input impedance;  $U_{3M}$  – operational amplifier's zero bias voltage;  $\Delta I$  – the difference between the operational amplifier's input currents;  $U_{III}$  – the noise voltage at the photodetector's output.

The output voltage module of noise is determined by expression [17, 18]:

$$(6) \quad U_{III} = \sqrt{E_{III}^2 + (I_{III}^2 + I_{III}^2 + I_{33}^2) R_{33}},$$

where  $E_{III}$  is the operational amplifier's noise voltage spectral density;  $I_{III}$  is the operational amplifier's noise current spectral density;  $I_{III}$  is the photodiode's noise current spectral density;  $I_{33}$  is the feedback connection's noise current resistance spectral density.

Photodiode's noise current density that operates in fotovoltaic mode [18]:

$$(7) \quad I_{III} = \sqrt{\frac{4kT\Delta f}{R_{VD}}},$$

where  $\Delta f$  is the effective band of electron path transmission.

The density of feedback connection's noise resistance current [18, 19]

$$(8) \quad I_{33} = \sqrt{\frac{4kT\Delta f}{R_{33}}}.$$

Taking into account the diode's and operational amplifier's mathematical models given in [20], (6) expression can be represented as follows:

$$(9) \quad \dot{U}_{\Phi} = \frac{FS_{I0} K_0 R_{BX} R_{33}}{1 + j\omega\tau_{VD}} \cdot \frac{E_{III}}{K_0 R_{BX} + R_{33} + R_{BX} - \frac{\omega^2 R_{BX} R_{33} (C_{BX} - C_{33})}{\omega_{TP}} + j\omega \left( \frac{(R_{33} + R_{BX})}{\omega_{TP}} + R_{BX} R_{33} (C_{BX} + C_{33} (K_0 + 1)) \right)}$$

where  $K_0$  is the operational amplifier's transmission factor at zero frequency;  $\omega_{TP}$  is the operational amplifier's maximum cyclic frequency.

In most cases, the photodiode's cutoff frequency is much lower than the operational amplifier's cutoff frequency [19, 21]. Therefore, the frequency response decrease in the high frequency range is determined by the photodiode's frequency properties. This makes it possible to ignore the parasitic capacitance's influence in the feedback circuit and the operational amplifier's input capacitance. The input resistance of modern operational amplifiers is tens of MOhms, which is much higher than the resistance in the feedback circuit and the photodiode's internal resistance [8]. Therefore it is possible to assume  $R_{BX} = \infty$ . Provided that the

irradiation frequency is much lower than the photodiode's cutoff frequency, its frequency properties can be neglected.

Given the above, (6) expression can be simplified:

$$(10) \quad U_{\Phi} = S_{I0}R_{33}F.$$

The linear dependence of the photodetector's output voltage on the luminous flux follows from (7) expression, which is the photodetector's simplified mathematical model based on a photodiode-operational amplifier pair. All the above assumptions are valid in our case, because the impurities' concentration cannot change instantly, and therefore the equivalent frequencies of the photodetector's output signal alternation will be quite low. Hence, by substituting (3) into (7) we will obtain:

$$(11) \quad U_{\Phi}(c) = S_{I0}R_{33}\alpha F_0 e^{-\varepsilon cd}.$$

Dependence (8) unambiguously connects the input and output values of proposed harmful impurities concentration optical sensor, being its conversion equation.

To obtain the proposed sensor's static characteristics, let us imagine the sensor's typical technical parameters: the photodiode's current sensitivity to selected radiation spectrum – 0.05 A/W, feedback resistance – 1kOhm, test gas's optical medium transparency coefficient – 0.8, the beam's luminous flux at the radiation source output – 0.1W, molar monochromatic absorption coefficient – 300 l/(mol·cm), the distance traveled by the beam – 20 cm, the molar concentration range – from 0 to  $10^{-4}$ , which roughly corresponds to volume concentration alteration range from 0 to 0.25% (maximum allowable carbon dioxide concentration in the livestock premises [1]). The static characteristics of the proposed sensor with the specified technical parameters are presented in Fig. 3.

As follows from Fig. 3, proposed sensor's static characteristic at selected technical parameters and specified measurement range is of a quasi-linear nature. The linearity of the sensor's static characteristics, in the general case, allows greatly to simplify the obtaining of the resulting transformation equation of the measuring instrument built on its basis. However, the linearization of quasi-linear dependence inevitably leads to increase in the methodological error [19, 22].

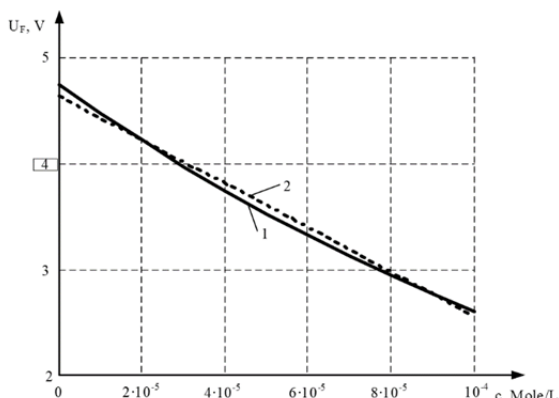


Fig. 3. Static characteristics of proposed contaminants concentration optical sensor :1 – derived from (11); 2 – linearized

Hence, to establish the feasibility of the obtained static characteristic's linearization, we will analyze the value of the additional methodological error that will be introduced as a result of linearization based on known relative measurement error's dependence:

$$(12) \quad \delta_{\delta}(c) = \frac{|U_{\Phi L}(c) - U_{\Phi}(c)|}{U_{\Phi}(c)} \cdot 100\%$$

where  $U_{\Phi L}(c)$  is the linearized dependence of voltage at the photodetector's output on the investigated impurity's molar concentration.

The results of modeling the dependence between relative linearization error and investigated impurity's molar concentration are shown in Fig. 4.

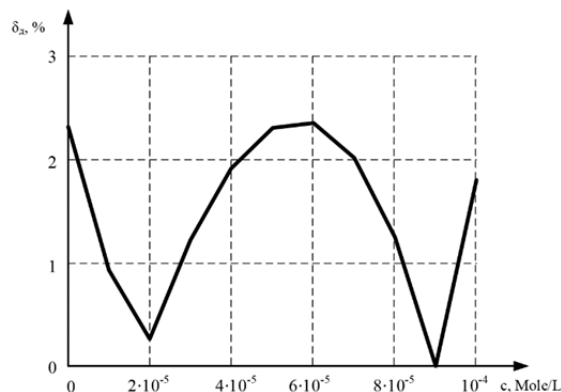


Fig. 4. Dependence between relative linearization error and investigated impurity's molar concentration

As follows from Fig. 4, the optical sensor's given values providing for acceptable sensitivity do not exceed 2.5%.

### Conclusion

1. Proposed was the design of the harmful air impurities' concentration optical sensor, which operation principle is based on application of Bouguer- Lambert-Beer effect suitable for operation in conjunction with an automated ventilation system.

2. Developed was the mathematical model of proposed sensor, on which basis the transformation equation was obtained. It has been demonstrated that within the measurement range, which corresponds to the change in controlled impurities ranging from zero to the maximum allowable concentration, the proposed sensor's static characteristic may represent an approximated linear function. The additional methodological error to be introduced due to linearization of the sensor's specified parameters does not exceed 2.5%.

**Authors:** GUNKO Irina – PhD in Engineering, Associate Professor, Vice-rector of the University to scientific and pedagogical work, Vinnytsia National Agrarian University (21008, 3 Sonyachna str., Vinnytsia, Ukraine); HRANIAK Valerii – PhD in Engineering, Associate Professor, Faculty of Engineering and Technology, Vinnytsia National Agrarian University (21008, 3 Sonyachna str., Vinnytsia, Ukraine, e-mail: [titanxp2000@ukr.net](mailto:titanxp2000@ukr.net)); YAROPUD Vitalii – PhD in Engineering, Associate Professor, Deputy Dean for pedagogical work, Faculty of Engineering and Technology, Vinnytsia National Agrarian University (21008, 3 Sonyachna str., Vinnytsia, Ukraine, e-mail: [yaropud77@gmail.com](mailto:yaropud77@gmail.com)); KUPCHUK Ihor – PhD in Engineering, Associate Professor, Deputy Dean for Scientific Research, Faculty of Engineering and Technology, Vinnytsia National Agrarian University (21008, 3 Sonyachna str., Vinnytsia, Ukraine, e-mail: [kupchuk.igor@i.ua](mailto:kupchuk.igor@i.ua)); RUTKEVYCH Volodymyr – PhD in Engineering, Associate Professor, Faculty of Engineering and Technology, Vinnytsia National Agrarian University (21008, 3 Sonyachna str., Vinnytsia, Ukraine).

### REFERENCES

- [1]. Yanovych V., Honcharuk T., Honcharuk I., Kovalova K. Engineering management of vibrating machines for targeted mechanical activation of premix components, *Inmateh-Agricultural Engineering*, 54 (2018), nr. 1, 25-32.

- [2]. Kupchuk I.M., Solona O.V., Derevenko I.A., Tverdokhlib I.V., Verification of the mathematical model of the energy consumption drive for vibrating disc crusher, *Inmateh – Agricultural Engineering*, 55 (2018), nr. 2, 111-118.
- [3]. Demchuk M. V., Chorny M. V., Zakharenko M. O., High M. P. Animal Hygiene. Textbook. Second edition. *Kharkiv: Espada*, 2006. 520 p.
- [4]. Bozhenko M. F. Heating, ventilation and air conditioning systems of buildings. *Kyiv: KPI named after Igor Sikorsky*, 2019. 380 p.
- [5]. Aliev E.B., Bandura V.M., Pryshliak V.M., Yaropud V.M., Trukhanska O.O. Modeling of mechanical and technological processes of the agricultural industry. *Inmateh–Agricultural Engineering*, 54 (2018), nr. 1, 95-32.
- [6]. Vedmitskiy Y. G., Kukharchuk V. V., Hraniak V. F., Vishtak I. V., Kacejko P., Abenov A. Newton binomial in the generalized Cauchy problem as exemplified by electrical systems. *Proceedings of SPIE 10808, Photonics Applications in Astronomy, Communications, Industry, and High-Energy Physics Experiments 2018 – 7* p. DOI: 10.1117/12.2501600.
- [7]. Yanovych, V., Honcharuk, T., Honcharuk, I., Kovalova, K. Design of the system to control a vibratory machine for mixing loose materials, *Eastern-European Journal of Enterprise Technologies*, 6 (2017), 4-13. DOI: 10.15587/1729-4061.2017.117635
- [8]. Golinko V. I., Romanenko V. I., Frundin V. E., Stasevich R. K., Control of oxygen and neodium gases in boiler emissions. *Municipal utilities. Scientific and technical collection*, 53 (2003), 115 – 118.
- [9]. Kuznietsova I., Bandura V., Paziuk V., Tokarchuk O., Kupchuk, I. Application of the differential scanning calorimetry method in the study of the tomato fruits drying process, *Agraarteadus*, 31 (2020), nr. 2, 173–180. DOI: 10.15159/jas.20.14.
- [10]. Vedmitskiy Y. G., Kukharchuk V. V., Hraniak V. F., New nonsystem physical quantities for vibration monitoring of transient processes at hydropower facilities, integral vibratory accelerations, *Przegląd Elektrotechniczny*, 93 (2017), nr.3, 69-72. DOI:10.15199/48.2017.03.17.
- [11]. Hraniak V. F., Kukharchuk V. V., Kucheruk V., Khassenov A. Using instantaneous cross-correlation coefficients of vibration signals for technical condition monitoring in rotating electric power machines, *Bulletin of the Karaganda University: PHYSICS Series*, 89 (2018), nr. 1, 72–80
- [12]. Lanets O., Derevenko I., Borovets V., Kovtonyuk M., Komada P., Mussabekov K., Yeraliyeva B. Substantiation of consolidated inertial parameters of vibrating bunker feeder, *Przegląd Elektrotechniczny*, 95 (2019), nr. 4, 47-52. DOI:10.15199/48.2019.04.09.
- [13]. Solona O., Kupchuk I. Dynamic synchronization of vibration exciters of the three-mass vibration mill, *Przegląd Elektrotechniczny*, 96 (2020), nr. 3, 163–167. DOI: 10.15199/48.2020.03.35.
- [14]. Honcharuk I., Kupchuk I., Solona O., Tokarchuk O., Telekalo N. Experimental research of oscillation parameters of vibrating-rotor crusher. *Przegląd Elektrotechniczny*, 97 (2021), nr. 3, 97–100. DOI: 10.15199/48.2021.03.19.
- [15]. Kulakov P. I. Mathematical model of a photovoltaic converter area-voltage based on a pair of photodiode-operational amplifier. *Proceedings of the Fifth International STC "Control and Management in Complex Systems*, 2 (1999), 228 – 233.
- [16]. Akseenko M. D., Baranochnikov M. L., Smolin O. V., Microelectronic photodetectors. *Moscow: Energoatomizdat*, 1984. 208 p.
- [17]. Kukharchuk V.V., Kazyv S.S., Bykovsky S.A., Discrete wavelet transformation in spectral analysis of vibration processes at hydropower units, *Przegląd Elektrotechniczny*, 93 (2017), Nr 5, 65-68
- [18]. Volkov V. A., Vyalov V. K., Gassanov L. G. and others; Under. Ed. L.Z. Kriksunov and L. S. Kremenchugsky. *Optical Receiver Handbook. Kyiv: Tehnika*, 1985. 216 p.
- [19]. Yanovych V., Kupchuk I., Determination of rational operating parameters for a vibrating disk-type grinder used in ethanol industry, *Inmateh – Agricultural Engineering*, 52 (2017), nr. 2, 143-148.
- [20]. Kulakov P. I., Gnes T. V. Mathematical model of an optical sensor for the presence of water in milk. *Optoelectronic information and energy technologies*, 1 (2012), 121 – 126.
- [21]. Horowitz P., Hill W., *The art of circuitry*. Translation from English. 2nd edition. *Moscow: BINOM*, 2014. 704 p.
- [22]. Posudin Y. I. *Methods of measuring environmental parameters. Kyiv: Svit*, 2003. 288 p.